Chemical Physics Letters 724 (2019) 1–7

Contents lists available at ScienceDirect

Chemical Physics Letters

journal homepage: www.elsevier.com/locate/cplett

Research paper

Controlling electronic properties of PtS_2/InSe van der Waals heterostructure via external electric field and vertical strain

Chuong V. Nguyen[a], H.D. Bui[b], Trinh D. Nguyen[c,d], Khang D. Pham[e,f,*]

[a] Department of Materials Science and Engineering, Le Quy Don Technical University, Ha Noi, Viet Nam
[b] Institute of Research and Development, Duy Tan University, Da Nang 550000, Viet Nam
[c] NTT Hi-Tech Institute, Nguyen Tat Thanh University, Ho Chi Minh City, Viet Nam
[d] Center of Excellence for Green Energy and Environmental Nanomaterials (CE@GrEEN), Nguyen Tat Thanh University, Ho Chi Minh City, Viet Nam
[e] Laboratory of Applied Physics, Advanced Institute of Materials Science, Ton Duc Thang University, Ho Chi Minh City, Viet Nam
[f] Faculty of Applied Sciences, Ton Duc Thang University, Ho Chi Minh City, Viet Nam

HIGHLIGHTS

- Electronic properties of PtS_2/InSe vdWH were investigated.
- PtS_2/InSe vdWH forms a type-II band alignment with an indirect band gap.
- Electronic properties of PtS_2/InSe vdWH can be controlled by strain and electric field.
- These findings suggest attractive potential application for PtS_2/InSe heterostructure as a novel optolectronic nanodevices.

ARTICLE INFO

Keywords:
DFT calculations
van der Waals heterostructures
Band gap controllable
Strain engineering
Electric field

ABSTRACT

In this letter, we systematically investigate the electronic properties of the PtS_2/InSe heterostructure using first-principle calculations. At the equilibrium interlayer distance D = 3.23 Å, the PtS_2/InSe heterostructure displays a semiconducting character with an indirect band gap. Moreover, it forms a type-II band alignment, making the PtS_2/InSe heterostructure a potential material for efficient separation of photogenerated electron-hole pairs. More interestingly, by applying vertical strain and electric field, the electronic properties of the PtS_2/InSe heterostructure can be effectively controlled, and a semiconductor-to-metal transition even emerges. These findings suggest attractive potential application for PtS_2/InSe heterostructure as a novel optolectronic nanodevices, along with a potential pholocatalyst.

1. Introduction

Since the discovery in 2004, graphene [1] has become one of the materials that has attracted both theoretical and experimental scientists due to its extraordinary physical properties [2–4]. However, the application of graphene to technology, especially in the field of optoelectronic nanodevices, still faces certain difficulties, in which the cause may be due to graphene having zero energy gap [5] and incompatibility between graphene and silicon electronic components. So far, there are many approaches to modulate the electronic states of graphene, i.e. to open a sizable gap around the Fermi level of graphene, that are stacking layers, electric field, doping, functionalization, edge effects [6–13].

In parallel with finding a way to overcome this limitation of graphene, a new research direction has emerged strongly in the last five years. That is looking for alternative materials. This new research has focused on two-dimensional (2D) materials such as phosphorene [14–23], transition metal dichalcogenides (TMDs) [24–28], hexagonal boron nitride (*h*-BN) [29] and post-transition metal chalcogenides (PTMCs) [30,31], and so on. Unlike graphene, these 2D materials are semiconductors with interesting properties and thus, they become potential candidate for applications in nanotechnology, such as photodetectors [32,33], field effect transistors (FETs) [32,34]. As a new member of the family of TMDs and PTMCs, 2D PtS_2 [35–37] and InSe [38–40] materials are gaining great attention due to their promising physical and chemical properties, which are favorable for furture applications in electronic and optoelectronic devices. It was shown that 2D PtS_2 material is a semiconductor with a layer-dependent indirect band gap, varying from 1.60 eV (1.80 eV) of monolayer to 0.25 eV

* Corresponding author at: Ton Duc Thang University, Ho Chi Minh City, Viet Nam.
E-mail address: phamdinhkhang@tdtu.edu.vn (K.D. Pham).

https://doi.org/10.1016/j.cplett.2019.03.048
Received 24 February 2019; Received in revised form 21 March 2019; Accepted 22 March 2019
Available online 25 March 2019

(0.48 eV) of bulk, obtained from experimental measurement (DFT calculation) [35]. Similar to 2D PtS_2 material, single-layer InSe has been synthesized experimentally [38] and its band gap depends strongly on the number of layers. Bulk InSe has a direct band gap, which can also transform to an indirect one of monolayer [41]. These properties of InSe material make it suitable for novel high-performance applications in optoelectronic devices, such as photodetectors and field-effect transistors (FETs) [42,43].

An another method currently being investigated is the creation of van der Waals (vdW) layered heterostructures from different 2D materials, thereby allowing for a better control of the electronic properties of these 2D materials. Layers of 2D materials are stacked to create large electric fields originating from the difference in work function. In addition, experimental and theoretical studies have shown that the major electronic properties of 2D materials are preserved due to the weak vdW interaction between layers in the heterostructures [44–48]. To date, there exists a large number of vdW heterostructures based on different 2D materials, such as graphene/TMDs [46,49–51], C_2N/Sb [52], PbI_2/BN [53], phosphorene/GaN [47], and so on. Very recently, TMDs/PTMCs vdW heterostructures, such as MoS_2/GaSe [54], MoS_2/InSe [55], GeSe/MoS_2 [56] and so on have been subjected to extensive investigations by theory and experiment. Chen et al. investigated the electronic properties of MoS_2/InSe vdW heterostructure. It was shown that such vdW heterostructure forms a type-II band alignment, which can be modulated by applying electric field or by changing the interlayer distance. To the best of our knowledge, up to now, there is no literature about the electronic properties of PtS_2/InSe vdW heterostructure as well as the effects of strain engineering and electric field on their properties.

Therefore, in this letter, we design a novel vdW heterostructure based on 2D PtS_2 and InSe monolayers and investigate the electronic properties of the PtS_2/InSe vdW heterostructure using first-principle calculations. In addition, the effects of the vertical strain and electric field on the electronic properties of heterostructure have also been considered.

2. Computational details

Our calculations of the geometric optimization and electronic properties were performed using the simulated Quantum Espresso package [57] through density functional theory (DFT). The Perdew-Burke-Ernzerhof (PBE) potential [58] of the generalized gradient approximation (GGA) [59] was used for describe the exchange-correlation energy. In addition, to describe correctly the weak vdW interactions, occurring between the different 2D PtS_2 and InSe layers, the London-dispersion corrected DFT-D2 method [60] was adopted. For the plane wave expansion, the cutoff energy was set to be 500 eV and the convergence thresholds between two steps were chosen as 10^{-6} and 10^{-3} eV/Å, respectively, for energy and force. We used a $9\times9\times1$ Monkhorst–Pack *k*-mesh to optimize the atomic structure and a $6\times6\times1$ *k*-mesh to calculate the electronic properties of the heterostructure. In addition, in order to avoid any interactions between neighboring slabs we set a large vacuum space of 25 Å along the *z* direction of the heterostructure.

3. Results and discussion

The atomic structure of the PtS_2/InSe HS was built by placing the PtS_2 ML on top of the InSe ML using a supercell, consisting of a (2×2) PtS_2 supercell and $(\sqrt{3}\times\sqrt{3})$ InSe supercell, as displayed in Fig. 1. Our calculated lattice mismatch between the PtS_2 and InSe supercell is very small and less than 2%, which show a little influence on the electronic characteristics of the PtS_2/InSe HS. Then, the geometric structure of the PtS_2/InSe HS was fully relaxed to obtain the equilibrium state with the obtained interlayer distance (D) in the PtS_2/InSe HS at the equilibrium state of 3.23 Å. Such distance indicates physical adsorption of the PtS_2 on the InSe layers in the heterostructure and shows a good agreement with that of other heterostructures based on 2D materials, such as MoS_2/SnS_2 [61], InSe/MoS_2 [55], graphene/phosphorene [47], SiGe/*h*-BN [62], which demonstrating the weak vdW interactions. In addition, we also check the stability of the PtS_2/InSe HS by performing the calculations of the binding energy as follows: $E_b = E_{PtS_2/InSe} - E_{PtS_2} - E_{InSe}$, where $E_{PtS_2/InSe}$, E_{PtS_2}, and E_{InSe}, respectively, are the total energies of the HS, isolated PtS_2 and InSe MLs. The obtained binding energy is −73.14 meV, which has the same order of magnitude as in other vdW heterostructures [63,64]. The more negative E_b, the systems are more stable and thus, could be easier to synthesize in experiments. Our obtained negative value of the E_b demonstrates that the HS is stable at the equilibrium state.

We now turn to evaluate the electronic properties of the PtS_2/InSe HS. As shown in Fig. 2, we can see that the PtS_2/InSe HS displays the semiconducting behavior with an indirect band gap of 1.21 eV at the equilibrium state. In addition, as compared with the band structures of the isolated PtS_2 and InSe MLs, we find that the PtS_2/InSe HS has a type-II band alignment. The lowest conduction band (CB) locates at the *M* point and comes from PtS_2 ML. Whereas, the highest valence band (VB) located at the Γ-M path and comes from the InSe ML. The band alignment of the PtS_2/InSe HS is illustrated in Fig. 3(a). The type-II band alignment makes the PtS_2/InSe HS potential material for applications in optoelectronics and photovoltaics, and it can be used as an electron-hole separator under photoexcitation. To have a more detailed understanding of the charge transfer between the PtS_2 and InSe MLs in the PtS_2/InSe HS, we further calculate the difference charge density, which can be calculated as follows: $\Delta\rho = \rho_{HS} - \rho_{PtS_2} - \rho_{InSe}$, where ρ_{HS}, ρ_{PtS_2}, and ρ_{InSe} are the charge densities of the HS, the isolated PtS_2 and InSe MLs, respectively. The difference charge density in the HS is displayed in Fig. 3(b). One can find that charges are depleted on the InSe layer and accumulated on PtS_2 layers.

When the heterostructure is applied to optoelectronic nanodevices, it can subject to electric field (E_{field}), which may cause a change in its electronic properties. Thus, it is interesting to consider whether the effect of an applied E_{field} affects the electronic properties of the PtS_2/InSe HS. The E_{field} is applied vertically along the stacked direction, i.e along the *z* direction, as illustrated in Fig. 4(a). The direction of applied E_{field}, pointing from the PtS_2 to the InSe layer is defined as the positive direction. The changes in the band edge positions (BEP) and the band gap of the PtS_2/InSe HS under different values of E_{field} is displayed in Fig. 4(b). We find that by increasing the E_{field} from −1 V/nm to +1 V/nm, the positions of the CB (Δ_{CB}) decrease dramatically, while the positions of the VB (Δ_{VB}) increases. In addition, the band gap of the PtS_2/InSe HS increases slightly with increasing the E_{field} from −1 V/nm to +1 V/nm. Interestingly, we find that when the applied E_{field} is smaller/larger than −1 V/nm/+1 V/nm, the $\Delta_{VB}/\Delta_{CB} < 0$, resulting in a transition from semiconductor to metal of the PtS_2/InSe HS.

In order to understand in detail the changes of the BEP and the band gap of the PtS_2/InSe HS under applied E_{field}, its band structures under different E_{field} are shown in Fig. 5. We find that the applied E_{field} affects the position of the Fermi level, thus, it results on the BEP of the PtS_2/InSe HS. When the positive E_{field} is subjected, the Fermi level is shifted downwards to the CB of the HS. The Δ_{VB}, thus, increases with increasing the applied positive E_{field}, whereas the Δ_{CB} decreases. More interestingly, under the applied positive E_{field} of +1 V/nm, we find that the CB of the PtS_2/InSe HS shifts upward to the Fermi level and crosses the Fermi level. Thus, the PtS_2/InSe HS displays a metallic trend, i.e a semiconductor-to-metal transition was occurred in the PtS_2/InSe HS when the positive E_{field} of +1 V/nm is subjected. On the contrary, when the negative E_{field} is subjected, it tends to shift the Fermi level towards the VB of the PtS_2/InSe HS. These things lead to an increase in the Δ_{CB} and to a decrease in the Δ_{VB}, as shown in Fig. 4(b). Furthermore, when the negative E_{field} of −1 V/nm is applied, the Δ_{VB} decreases to 0.07 eV. Our results show that the Δ_{VB} continuously decreases and achieves zero with the increasing E_{field} down to −1.2 V/nm. It indicates that a

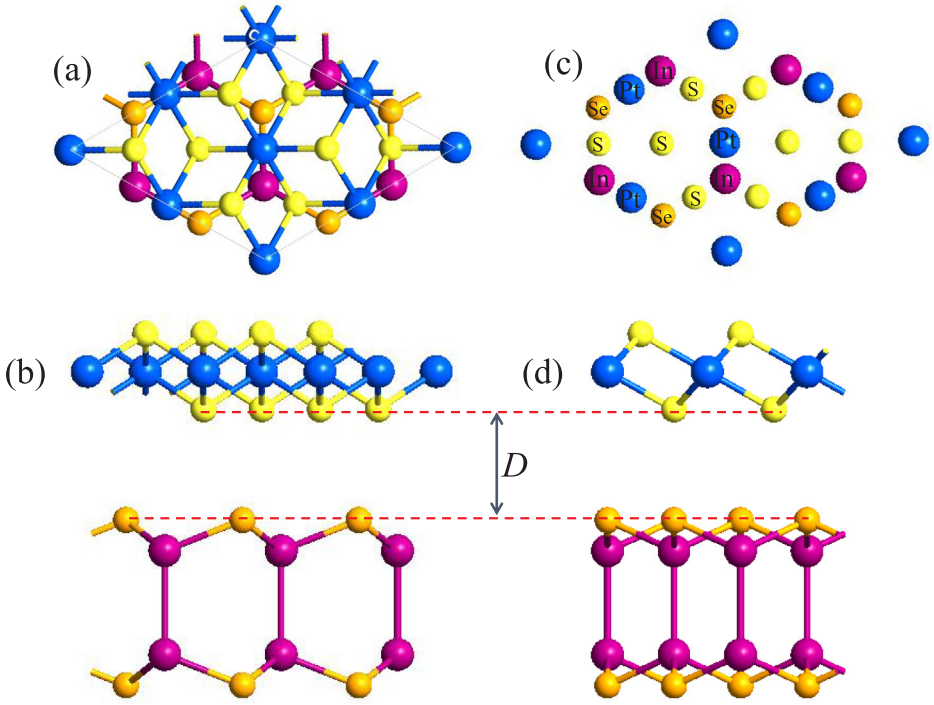

Fig. 1. (a) and (c) Top view, (b) and (d) side view of the atomic structure of the PtS_2/InSe HS.

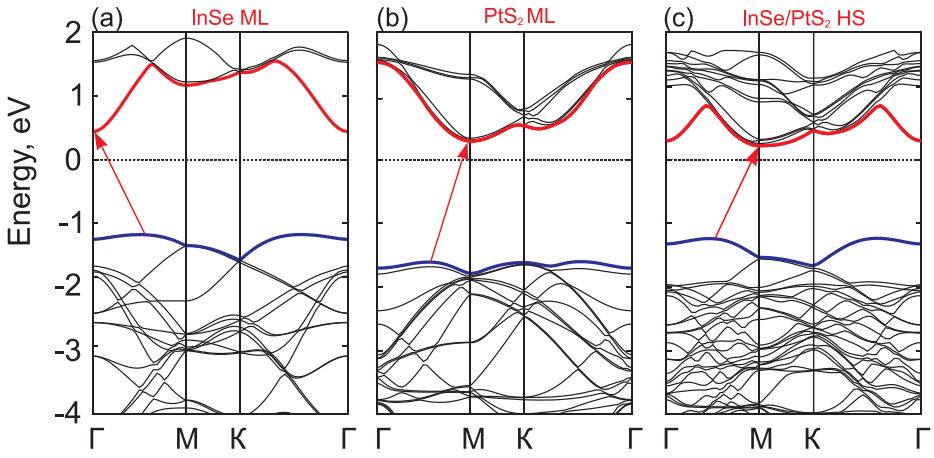

Fig. 2. Calculated band structures of the isolated InSe (a), PtS_2 (b) monolayers and (c) PtS_2/InSe HS.

semiconductor-to-metal transition of the PtS_2/InSe HS is observed when the negative E_{field} of −1.2 V/nm is applied. Also, one can observe that the positive and negative E_{field} affects differently the electronic properties of the PtS_2/InSe HS owing to the spontaneous electric polarization, which may originate from the electronegativity difference between S and Se layers. Thus, the electrons and holes in the PtS_2/InSe HS are localized separately at the S and Se layers, respectively.

Furthermore, the vertical strain by changing the interlayer coupling between two different layered materials in their vdW heterostructures is well known to be an effective method to modulate the electronic properties, which may enhance the electronic device performances [65–68]. Besides, it can be seen that controlling the interlayer spacing D in the vdWHS can be easily performed in experiments by various methods, such as pressure [69], insertion of the dielectric layers [70]. Thus, it is interesting to explore the effect of the vertical strain on the electronic properties of the PtS_2/InSe HS, as illustrated in Fig. 6(a). Fig. 6(b) shows the evolution of the BEP and the band gap size of the PtS_2/InSe HS as functions of the D. One can find that with increasing the D from 2.53 Å to 4.13 Å, the band gap size of the PtS_2/InSe HS slightly increases from 1.24 eV to 1.45 eV, respectively, as shown in Fig. 6(b). Also, with increasing the D, the position of the VB (Δ_{VB}) decreases, while the position of the CB (Δ_{CB}) increases accordingly, as shown in Fig. 6(b). For instance, when we decreased the D from 4.13 Å to 3.23 Å and then to 2.53 Å, the Δ_{VB} increases from 0.25 eV to 1.10 eV and then to 1.17 eV, respectively, while the Δ_{CB} decreases from 1.19 eV to 0.21 eV and then to 0.04 eV, respectively. Interestingly, our results demonstrate that the semiconductor-to-metal can be achieved in the PtS_2/InSe HS when the D is smaller than 2.53 Å. Such transition plays an important role in the field of optoelectronic nanodevices.

To get further insights into the band structures modulation of the PtS_2/InSe HS, in Fig. 7 we plot its band structures under different D. Under vertical strain, a semiconducting character with an indirect band gap is maintained in the Pt_2/InSe HS. The band gap increases slightly with increasing the D. When the D is reached 4.13 Å, it can be seen from Fig. 7(f) that the CB of such vdWHS is shifted from the M to the Γ point, whereas its VB is still located at the Γ-M path. Moreover, with increasing the D, the Fermi level shifts upwards from the CB to the VB of the PtS_2/InSe HS. It leads to a/an decrease/increase in the Δ_{VB}/Δ_{CB}.

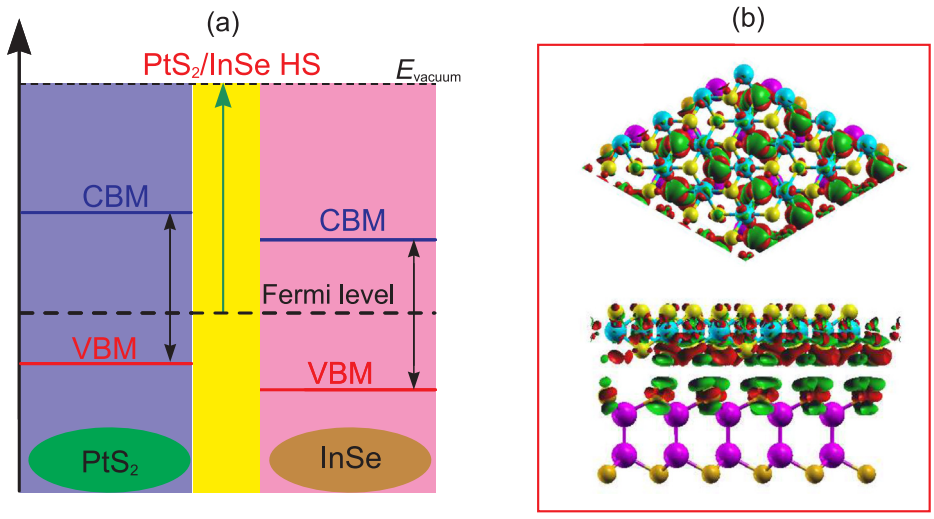

Fig. 3. (a) Band alignment and the difference charge density of PtS_2/InSe HS along the *z* direction. The red and green regions represent electrons accumulation and depletion, respectively. (For interpretation of the references to colour in this figure legend, the reader is referred to the web version of this article.)

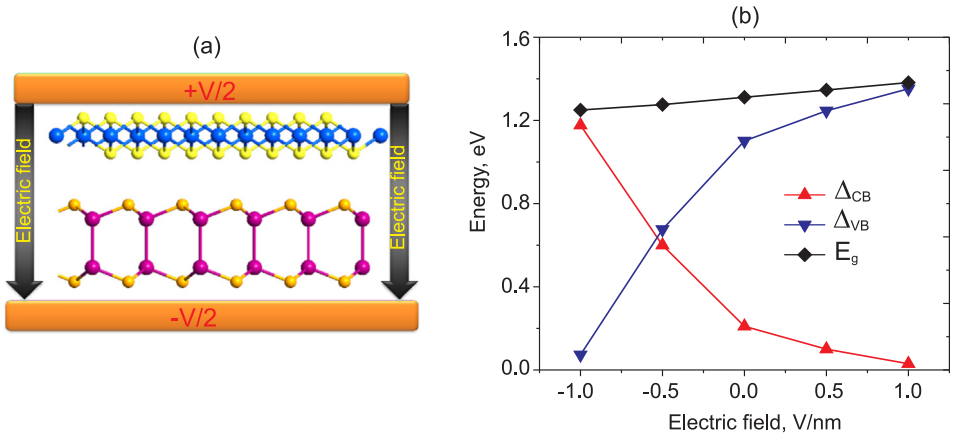

Fig. 4. (a) Schematic model of applied E_{field}. (b) The position of the CB, VB and the band gap of the PtS_2/InSe HS as functions of the E_{field}.

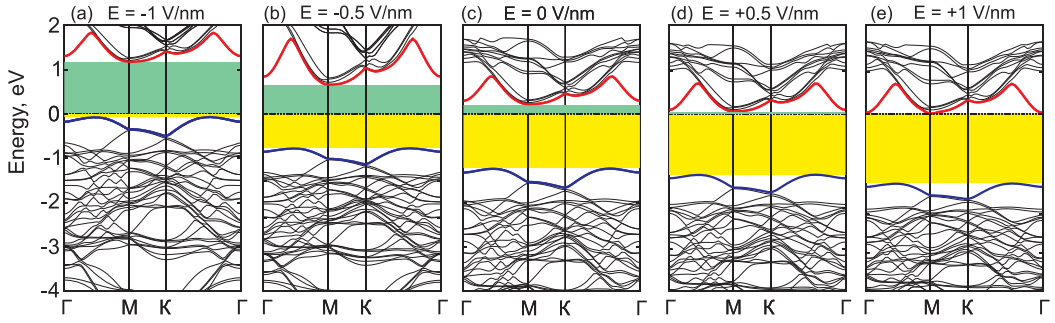

Fig. 5. Band structures of the PtS_2/InSe HS with applied E_{field} of −1 V/nm (a), −0.5 V/nm (b), 0 V/nm (c), +0.5 V/nm, (d) +1 V/nm.

When the *D* is smaller than 2.53 Å, the CB of the vdWHS moves upwards and crosses the Fermi level, showing a semiconductor-to-metal transition. These results suggest attractive potential application for the Pt_2/InSe HS with tunable interlayers as a novel optoelectronic nanodevices, along with a potential pholocatalyst. Finally, it should be noted that the PtS_2/InSe vdWH has not yet been synthesized in experiments. However, numerical vertical heterostructures based on MX_2 and MX monolayers, such as $MoSe_2$/GaSe, MoS_2/GaSe has recently been synthesized in experiments via van der Waals epitaxy [71] or chemical vapor deposition (CVD) method [54]. Thus, we believe that the PtS_2/InSe can be realized by stacking exfoliated, chemical vapor deposition (CVD) or vdW epitaxy in the near future.

4. Conclusions

In summary, we investigated the electronic properties of PtS_2/InSe van der Waals heterostructure under vertical strain and electric field through first-principle calculations. Our results reveals that the weak vdW interactions are dominated in the PtS_2/InSe HS, which has a negative binding energy of −73.14 meV at the equilibrium interlayer distance $D = 2.32$ Å. The PtS_2/InSe HS possesses a semiconducting behavior with a direct band gap of 1.21 eV and forms a type-II band alignment, which may acceptable for efficient separation of photogenerated electron-hole pairs. Moreover, the electronic properties of the PtS_2/InSe HS can be effectively modulated under external electric

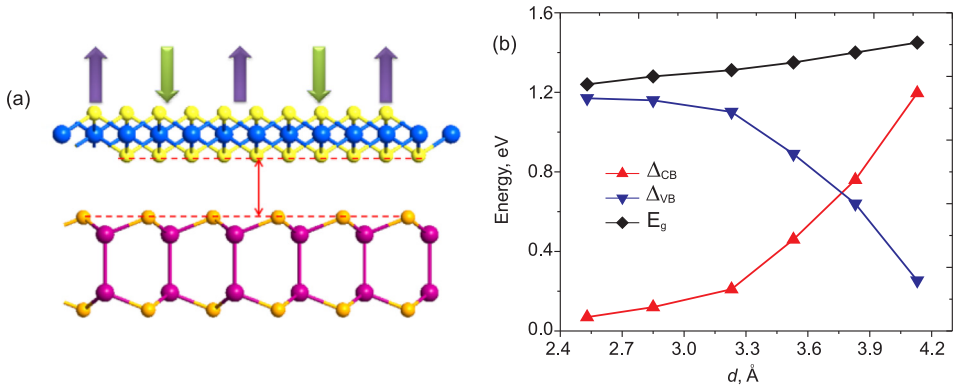

Fig. 6. (a) Schematic model of applied out-of-plane strain. (b) The position of the CB, VB and the band gap of the PtS_2/InSe HS as functions of the D.

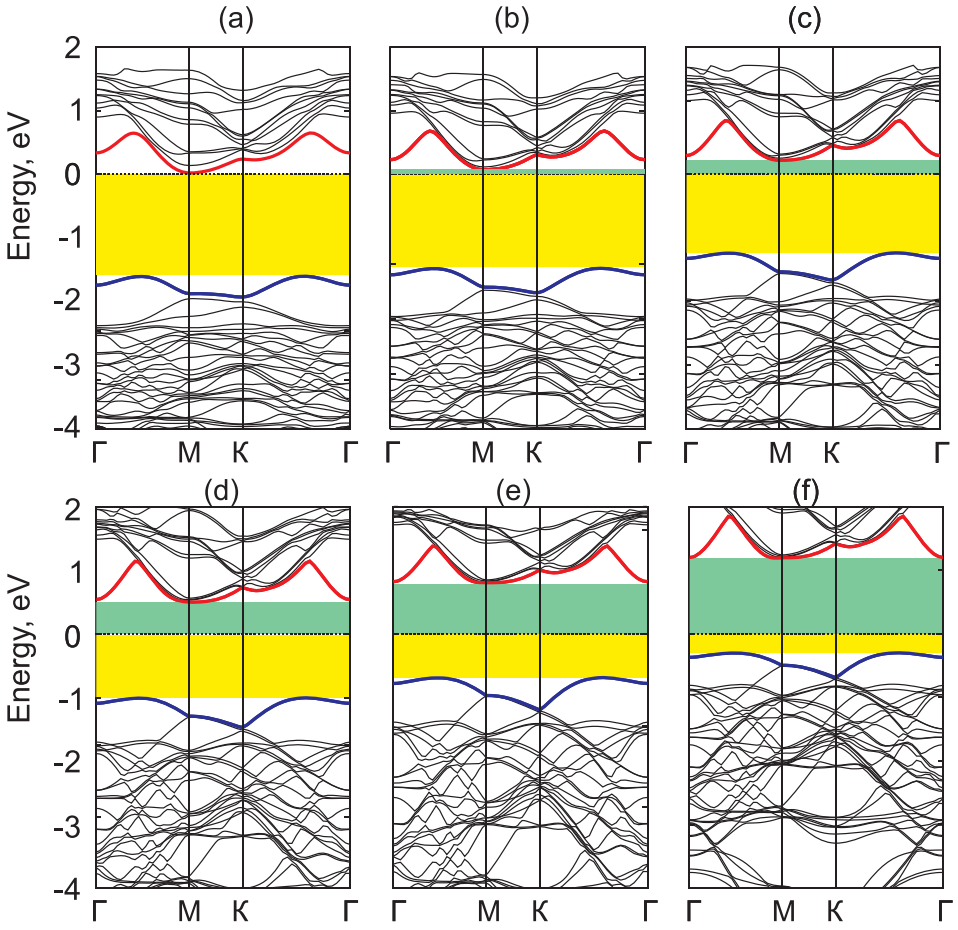

Fig. 7. Band structures of the PtS_2/InSe HS under different D of (a) 2.53 Å, (b) 2.83 Å, (c) 3.23 Å, (d) 3.53 Å, (e) 3.83 Å, and (f) 4.13 Å.

field and vertical strain. When an electric field is applied, such heterostructure emerges a semiconductor-to-metal at the $E_{field} = -1.2$ V/nm. Whereas, when the HS is subjected to the vertical strain, a transition from semiconductor to metal occurs at the $D = 2.50$ Å. These results demonstrate that the PtS_2/InSe HS can become a promising material for applications in next-generation electronic and optoelectronic devices.

Conflict of interest

The authors declared that there is no conflict of interest.

References

[1] K.S. Novoselov, A.K. Geim, S.V. Morozov, D. Jiang, Y. Zhang, S.V. Dubonos, I.V. Grigorieva, A.A. Firsov, Electric field effect in atomically thin carbon films, Science 306 (5696) (2004) 666–669.
[2] Y.-M. Lin, C. Dimitrakopoulos, K.A. Jenkins, D.B. Farmer, H.-Y. Chiu, A. Grill, P. Avouris, 100-GHz transistors from wafer-scale epitaxial graphene, Science 327 (2010) 662.
[3] L. Ponomarenko, R. Yang, T. Mohiuddin, M. Katsnelson, K. Novoselov, S. Morozov, A. Zhukov, F. Schedin, E. Hill, A. Geim, Effect of a high-κ environment on charge carrier mobility in graphene, Phys. Rev. Lett. 102 (2009) 206603.
[4] X. Du, I. Skachko, A. Barker, E.Y. Andrei, Approaching ballistic transport in suspended graphene, Nat. Nanotechnol. 3 (2008) 491.
[5] K.S. Novoselov, A.K. Geim, S. Morozov, D. Jiang, M. Katsnelson, I. Grigorieva, S. Dubonos, A. Firsov, Two-dimensional gas of massless dirac fermions in graphene, Nature 438 (2005) 197.
[6] N.D. Hien, K. Mirabbaszadeh, M. Yarmohammadi, B.D. Hoi, Linear magneto-

electron-light interaction in ultranarrow armchair graphene and boronitrene nanoribbons, Diamond Related Mater. 92 (2019) 86–91.
[7] M. Sun, Y. Peng, Study on structural, electronic and magnetic properties of sn atom adsorbed on defective graphene by first-principle calculations, Appl. Surf. Sci. 307 (2014) 158–164.
[8] P. Le, K. Mirabbaszadeh, M. Yarmohammadi, Magneto-EELS of armchair boronitrene nanoribbons, RSC Adv. 9 (2019) 2829–2835.
[9] M. Sun, W. Tang, Q. Ren, S. Wang, Y. Du, Y. Zhang, et al., First-principles study of the alkali earth metal atoms adsorption on graphene, Appl. Surf. Sci. 356 (2015) 668–673.
[10] P.T. Le, M. Davoudiniya, M. Yarmohammadi, Interplay of orbital hopping and perpendicular magnetic field in anisotropic phase transitions for bernal bilayer graphene and hexagonal boron-nitride, Phys. Chem. Chem. Phys. 21 (2019) 238–245.
[11] M. Yarmohammadi, Impurity doping effects on the orbital thermodynamic properties of hydrogenated graphene, graphane, in harrison model, Phys. Lett. A 380 (2016) 4062–4069.
[12] B.D. Hoi, M. Yarmohammadi, Combined effect of the perpendicular magnetic field and dilute charged impurity on the electronic phase of bilayer aa-stacked hydrogenated graphene, Phys. Lett. A 382 (2018) 3298–3305.
[13] M. Yarmohammadi, Perturbation tuning of plasmon modes in semiconductor armchair nanoribbons, Phys. Rev. B 98 (2018) 155424.
[14] H. Liu, A.T. Neal, Z. Zhu, Z. Luo, X. Xu, D. Tománek, P.D. Ye, Phosphorene: an unexplored 2D semiconductor with a high hole mobility, ACS Nano 8 (2014) 4033–4041.
[15] P. Le, M. Yarmohammadi, Anisotropic magneto-thermoelectric properties of single-layer dilute charged impurity-infected black phosphorus, Physica E 107 (2019) 11–17.
[16] H. Bui, M. Yarmohammadi, Direction-dependent electronic phase transition in magnetic field-induced gated phosphorene, J. Magn. Magn. Mater. 465 (2018) 646–650.
[17] E. Samuel Reich, Phosphorene excites materials scientists, Nature News 506 (2014) 19.
[18] P. Le, K. Mirabbaszadeh, M. Davoudiniya, M. Yarmohammadi, Charged impurity-tuning of midgap states in biased bernal bilayer black phosphorus: an anisotropic electronic phase transition, Phys. Chem. Chem. Phys. 20 (2018) 25044–25051.
[19] D. Bui, M. Yarmohammadi, Impurity-induced anisotropic semiconductor-semimetal transition in monolayer biased black phosphorus, Phys. Lett. A 382 (2018) 1885–1889.
[20] H. Bui, M. Yarmohammadi, Pauli magnetic susceptibility of doped and biased phosphorene in the presence of zeeman magnetic field and dilute charged impurity, Superlatt. Microstruct. 122 (2018) 453–460.
[21] M. Sun, S. Wang, J. Yu, W. Tang, Hydrogenated and halogenated blue phosphorene as Dirac materials: a first principles study, Appl. Surf. Sci. 392 (2017) 46–50.
[22] P. Le, M. Davoudiniya, K. Mirabbaszadeh, B. Hoi, M. Yarmohammadi, Combined electric and magnetic field-induced anisotropic tunable electronic phase transition in AB-stacked bilayer phosphorene, Physica E 106 (2019) 250–257.
[23] H. Bui, L.T. Phuong, M. Yarmohammadi, On the influence of dilute charged impurity and perpendicular electric field on the electronic phase of phosphorene: Band gap engineering, Europhys. Lett. 124 (2018) 27001.
[24] Q.H. Wang, K. Kalantar-Zadeh, A. Kis, J.N. Coleman, M.S. Strano, Electronics and optoelectronics of two-dimensional transition metal dichalcogenides, Nat. Nanotechnol. 7 (2012) 699.
[25] M. Yarmohammadi, The effects of strain on dc transverse and spin-valley hall conductivity of ferromagnetic MoS_2 and silicene, J. Magn. Magn. Mater. 426 (2017) 621–628.
[26] M. Chhowalla, H.S. Shin, G. Eda, L.-J. Li, K.P. Loh, H. Zhang, The chemistry of two-dimensional layered transition metal dichalcogenide nanosheets, Nat. Chem. 5 (2013) 263.
[27] M. Yarmohammadi, Role of spin-orbit interaction and impurity doping in thermodynamic properties of monolayer MoS_2, J. Elect. Mater. 45 (2016) 4958–4965.
[28] P. Johari, V.B. Shenoy, Tuning the electronic properties of semiconducting transition metal dichalcogenides by applying mechanical strains, ACS Nano 6 (2012) 5449–5456.
[29] B.D. Hoi, M. Yarmohammadi, Zeeman-magnetic-field-induced magnetic phase transition in doped armchair boron-nitride nanoribbons, Europhys. Lett. 122 (2018) 17005.
[30] S. Demirci, N. Avazlı, E. Durgun, S. Cahangirov, Structural and electronic properties of monolayer group III monochalcogenides, Phys. Rev. B 95 (2017) 115409.
[31] A.K. Singh, R.G. Hennig, Computational prediction of two-dimensional group-IV mono-chalcogenides, Appl. Phys. Lett. 105 (2014) 042103.
[32] L. Li, Y. Yu, G.J. Ye, Q. Ge, X. Ou, H. Wu, D. Feng, X.H. Chen, Y. Zhang, Black phosphorus field-effect transistors, Nat. Nanotechnol. 9 (2014) 372.
[33] C. Xie, C. Mak, X. Tao, F. Yan, Photodetectors based on two-dimensional layered materials beyond graphene, Adv. Funct. Mater. 27 (2017) 1603886.
[34] V. Podzorov, M. Gershenson, C. Kloc, R. Zeis, E. Bucher, High-mobility field-effect transistors based on transition metal dichalcogenides, Appl. Phys. Lett. 84 (2004) 3301–3303.
[35] Y. Zhao, J. Qiao, P. Yu, Z. Hu, Z. Lin, S.P. Lau, Z. Liu, W. Ji, Y. Chai, Extraordinarily strong interlayer interaction in 2D layered PtS_2, Adv. Mater. 28 (2016) 2399–2407.
[36] M. Sajjad, N. Singh, U. Schwingenschlögl, Strongly bound excitons in monolayer PtS_2 and $PtSe_2$, Appl. Phys. Lett. 112 (2018) 043101.
[37] G. Liu, Y. Gan, R. Quhe, P. Lu, Strain dependent electronic and optical properties of PtS_2 monolayer, Chem. Phys. Lett. 709 (2018) 65–70.
[38] W. Huang, L. Gan, H. Li, Y. Ma, T. Zhai, 2d layered group IIIA metal chalcogenides: synthesis, properties and applications in electronics and optoelectronics, CrystEngComm 18 (2016) 3968–3984.
[39] K. Xu, L. Yin, Y. Huang, T.A. Shifa, J. Chu, F. Wang, R. Cheng, Z. Wang, J. He, Synthesis, properties and applications of 2D layered $M^{III}X^{VI}$ (M = Ga, In; X = S, Se, Te) materials, Nanoscale 8 (2016) 16802–16818.
[40] S.J. Magorrian, V. Zólyomi, V.I. Fal'ko, Electronic and optical properties of two-dimensional InSe from a DFT-parametrized tight-binding model, Phys. Rev. B 94 (2016) 245431.
[41] C. Sun, H. Xiang, B. Xu, Y. Xia, J. Yin, Z. Liu, Ab initio study of carrier mobility of few-layer InSe, Appl. Phys. Exp. 9 (2016) 035203.
[42] S. Sucharitakul, N.J. Goble, U.R. Kumar, R. Sankar, Z.A. Bogorad, F.-C. Chou, Y.-T. Chen, X.P. Gao, Intrinsic electron mobility exceeding 10^3 $cm^2/(Vs)$ in multilayer inse fets, Nano Lett. 15 (2015) 3815–3819.
[43] S.R. Tamalampudi, Y.-Y. Lu, R. Kumar U, R. Sankar, C.-D. Liao, K. Moorthy B, C.-H. Cheng, F.C. Chou, Y.-T. Chen, High performance and bendable few-layered inse photodetectors with broad spectral response, Nano Lett. 14 (2014) 2800–2806.
[44] F. Yan, L. Zhao, A. Patanè, P. Hu, X. Wei, W. Luo, D. Zhang, Q. Lv, Q. Feng, C. Shen, et al., multicolor photodetection with graphene-contacted p-GaSe/n-InSe van der Waals heterostructures, Nanotechnology 28 (2017) 27LT01.
[45] W. Zhang, D. Chang, Q. Gao, C. Niu, C. Li, F. Wang, X. Huang, C. Xia, Y. Jia, Interlayer coupling and external electric field tunable electronic properties of a 2D type-I α-tellurene/MoS_2 heterostructure, J. Mater. Chem. C 6 (2018) 10256–10262.
[46] D. Pierucci, H. Henck, J. Avila, A. Balan, C.H. Naylor, G. Patriarche, Y.J. Dappe, M.G. Silly, F. Sirotti, A.C. Johnson, et al., Band alignment and minigaps in monolayer MoS_2-graphene van der waals heterostructures, Nano Lett. 16 (2016) 4054–4061.
[47] M. Sun, J.-P. Chou, J. Yu, W. Tang, Electronic properties of blue phosphorene/graphene and blue phosphorene/graphene-like gallium nitride heterostructures, Phys. Chem. Chem. Phys. 19 (2017) 17324–17330.
[48] Y. Luo, S. Wang, K. Ren, J.-P. Chou, J. Yu, Z. Sun, M. Sun, Transition-metal dichalcogenides/$Mg(OH)_2$ van der Waals heterostructures as promising water-splitting photocatalysts: a first-principles study, Phys. Chem. Chem. Phys. 21 (2019) 1791–1796.
[49] K. Kim, S. Larentis, B. Fallahazad, K. Lee, J. Xue, D.C. Dillen, C.M. Corbet, E. Tutuc, Band alignment in WSe_2-graphene heterostructures, ACS Nano 9 (2015) 4527–4532.
[50] Z.B. Aziza, H. Henck, D. Di Felice, D. Pierucci, J. Chaste, C.H. Naylor, A. Balan, Y.J. Dappe, A.C. Johnson, A. Ouerghi, Bandgap inhomogeneity of MoS_2 monolayer on epitaxial graphene bilayer in van der waals pn junction, Carbon 110 (2016) 396–403.
[51] M. Kuiri, B. Chakraborty, A. Paul, S. Das, A. Sood, A. Das, Enhancing photoresponsivity using $MoTe_2$-graphene vertical heterostructures, Appl. Phys. Lett. 108 (2016) 063506.
[52] X. Wang, R. Quhe, W. Cui, Y. Zhi, Y. Huang, Y. An, X. Dai, Y. Tang, W. Chen, Z. Wu, et al., Electric field effects on the electronic and optical properties in C_2N/Sb van der Waals heterostructure, Carbon 129 (2018) 738–744.
[53] Y. Ma, X. Zhao, M. Niu, X. Dai, W. Li, X. Wang, M. Zhao, T. Wang, Y. Tang, Modulation of interfacial electronic properties in PbI_2 and BN van der Waals heterobilayer via external electric field, Appl. Surf. Sci. 411 (2017) 46–52.
[54] N. Zhou, R. Wang, X. Zhou, H. Song, X. Xiong, Y. Ding, J. Lü, L. Gan, T. Zhai, P-GaSe/N-MoS_2 vertical heterostructures synthesized by van der waals epitaxy for photoresponse modulation, Small 14 (2018) 1702731.
[55] X. Chen, Z.-Z. Lin, M. Ju, Controllable band alignment transition in InSe–MoS_2 Van der Waals heterostructure, Phys. Status Solidi Rapid Res. Lett. 12 (2018) 1800102.
[56] D. Tan, X. Wang, W. Zhang, H.E. Lim, K. Shinokita, Y. Miyauchi, M. Maruyama, S. Okada, K. Matsuda, Carrier transport and photoresponse in GeSe/MoS_2 heterojunction p–n diodes, Small 14 (2018) 1704559.
[57] P. Giannozzi, S. Baroni, N. Bonini, M. Calandra, R. Car, C. Cavazzoni, D. Ceresoli, G.L. Chiarotti, M. Cococcioni, I. Dabo, A.D. Corso, S. de Gironcoli, S. Fabris, G. Fratesi, R. Gebauer, U. Gerstmann, C. Gougoussis, A. Kokalj, M. Lazzeri, L. Martin-Samos, N. Marzari, F. Mauri, R. Mazzarello, S. Paolini, A. Pasquarello, L. Paulatto, C. Sbraccia, S. Scandolo, G. Sclauzero, A.P. Seitsonen, A. Smogunov, P. Umari, R.M. Wentzcovitch, QUANTUM ESPRESSO: a modular and open-source software project for quantum simulations of materials, J. Phys.: Condens. Matter 21 (2009) 395502–395520.
[58] J.P. Perdew, K. Burke, M. Ernzerhof, Perdew, burke, and ernzerhof reply, Phys. Rev. Lett. 80 (1998) 891.
[59] J.P. Perdew, K. Burke, M. Ernzerhof, Generalized gradient approximation made simple, Phys. Rev. Lett. 77 (1996) 3865.
[60] S. Grimme, Semiempirical GGA-type density functional constructed with a long-range dispersion correction, J. Comput. Chem. 27 (2006) 1787–1799.
[61] D.S. Koda, F. Bechstedt, M. Marques, L.K. Teles, Trends on band alignments: validity of anderson's rule in SnS_2- and $SnSe_2$-based van der Waals heterostructures, Phys. Rev. B 97 (2018) 165402.
[62] X. Chen, X. Sun, D. Yang, R. Meng, C. Tan, Q. Yang, Q. Liang, J. Jiang, SiGe/h-BN heterostructure with inspired electronic and optical properties: a first-principles study, J. Mater. Chem. C 4 (2016) 10082–10089.
[63] S. Wang, C. Ren, H. Tian, J. Yu, M. Sun, MoS_2/ZnO van der Waals heterostructure as a high-efficiency water splitting photocatalyst: a first-principles study, Phys. Chem. Chem. Phys. 20 (2018) 13394–13399.
[64] M. Luo, Y. Xu, Y. Song, Tunable electronic properties of MoS_2/ReS_2 van der waals heterostructure from first-principles study, Optik 144 (2017) 334–339.
[65] J. Shang, L. Pan, X. Wang, J. Li, H.-X. Deng, Z. Wei, Tunable electronic and optical properties of InSe/InTe van der waals heterostructures toward optoelectronic applications, J. Mater. Chem. C 6 (2018) 7201–7206.
[66] K.D. Pham, N.N. Hieu, H.V. Phuc, I. Fedorov, C. Duque, B. Amin, C.V. Nguyen, Layered graphene/GaS van der waals heterostructure: controlling the electronic

properties and schottky barrier by vertical strain, Appl. Phys. Lett. 113 (2018) 171605.
[67] M. Sun, J.-P. Chou, Q. Ren, Y. Zhao, J. Yu, W. Tang, Tunable schottky barrier in van der waals heterostructures of graphene and g-GaN, Appl. Phys. Lett. 110 (2017) 173105.
[68] F. Zhang, W. Li, Y. Ma, X. Dai, Strain effects on the schottky contacts of graphene and $MoSe_2$ heterobilayers, Physica E 103 (2018) 284–288.
[69] M. Dienwiebel, G.S. Verhoeven, N. Pradeep, J.W.M. Frenken, J.A. Heimberg, H.W. Zandbergen, Superlubricity of graphite, Phys. Rev. Lett. 92 (2004) 126101.
[70] H. Fang, C. Battaglia, C. Carraro, S. Nemsak, B. Ozdol, J.S. Kang, H.A. Bechtel, S.B. Desai, F. Kronast, A.A. Unal, G. Conti, C. Conlon, G.K. Palsson, M.C. Martin, A.M. Minor, C.S. Fadley, E. Yablonovitch, R. Maboudian, A. Javey, Strong interlayer coupling in van der waals heterostructures built from single-layer chalcogenides, Proc. Nat. Acad. Sci. 111 (2014) 6198–6202.
[71] X. Li, M.-W. Lin, J. Lin, B. Huang, A.A. Puretzky, C. Ma, K. Wang, W. Zhou, S.T. Pantelides, M. Chi, I. Kravchenko, J. Fowlkes, C.M. Rouleau, D.B. Geohegan, K. Xiao, Two-dimensional GaSe/$MoSe_2$ misfit bilayer heterojunctions by van der waals epitaxy, Sci. Adv. 2 (2016) e1501882.